RSC Advances



This is an *Accepted Manuscript*, which has been through the Royal Society of Chemistry peer review process and has been accepted for publication.

Accepted Manuscripts are published online shortly after acceptance, before technical editing, formatting and proof reading. Using this free service, authors can make their results available to the community, in citable form, before we publish the edited article. This Accepted Manuscript will be replaced by the edited, formatted and paginated article as soon as this is available.

You can find more information about *Accepted Manuscripts* in the **Information for Authors**.

Please note that technical editing may introduce minor changes to the text and/or graphics, which may alter content. The journal's standard <u>Terms & Conditions</u> and the <u>Ethical guidelines</u> still apply. In no event shall the Royal Society of Chemistry be held responsible for any errors or omissions in this *Accepted Manuscript* or any consequences arising from the use of any information it contains.



RSC Advances

Cite this: DOI: 10.1039/c3dt00000x

www.rsc.org/ RSC Advances

PAPER

Syntheses, crystal structures, photoluminescent/magnetic properties of four new coordination polymers based on 2,3°, 4,5°-biphenyltetracarboxylic acid†

Jin-Zhong Qiao, ^{1a} Mao-Sheng Zhan, ^a and Tuo-Ping Hu*^b

5 **ABSTRACT:** Hydrothermal reactions of 2,3',4,5'-biphenyltetracarboxylic acid (H₄bptc) with divalent copper, cobalt and nickel salts afford four novel coordination polymers, namely, {[Cu_{2.5}(μ₃-OH)(bptc⁴)(4,4'-bpy)(H₂O)]·1.5H₂O}_n(1), {[Cu₂(bptc⁴)(H₂O)₄]·4H₂O}_n(2), {[Co_{1.5}(Hbptc³)(1,4-bib)_{0.5}(H₂O)₅]·2H₂O}_n(3), and {[Ni₂(bptc⁴)(1,4-bib)_{1.5}(H₂O)₅]·5H₂O}_n(4), in the presence of ancillary ligands (4,4'-bpy = 4,4'-bipyridine, 1,4-bib = 1,4-bis(1-imidazolyl)benzene). Their structures were determined by single-crystal X-ray diffraction analyses and further characterized by IR spectra, elemental analyses, powder X-ray diffraction (PXRD), thermogravimetric (TG) analyses. Complex 1 exhibits a 3D framework with one-dimensional channels along the [111] direction, which can be defined as a (4,10)-connected deh1 net with the point Schläfli symbol of {3·4⁵}₂{3⁴·4¹²·5¹⁰·6¹⁴·7³·8²}. Compound 2 contains two interpenetrated 3D networks, each of which can be viewed as a (4,4)-connected mog Moganite network with the point Schläfli symbol of {4·6·4⁸}₂{4²·6²·8²}. In Complex 3, both the Hbptc³⁻ and the 1,4-bib show μ₂ coordination mode, the former of which links two Co2 cations to form a 1D anionic chain and the latter of which links two Co1 cations to generate a 1D cationic chain. Interestingly, the 1D anionic chains are assembled through abundant strong hydrogen bonds to generate a 3D supermolecular structure with large one-dimensional channels occupied by the 1D cationic chains along the *c* axis. Complex 4 consists of two interpenetrated 3D networks, each of which can be simplified as a novel (3,4,4)-connected framework with the point Schläfli symbol of {4·6·8} {4·6³·8²} {6⁴·8·10}. In addition, the magnetic properties for 1, 2 and the photoluminescent properties for 3, 4 were investigated. The magnetic results show that there exist antiferromagnetic interactions between Cu(II) ions in 1 and 2.

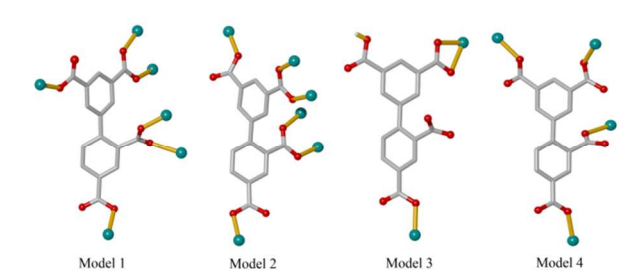
20 Introduction

Coordination polymers (CPs) have become increasingly attractive organic-inorganic hybrid materials with appealing structure and novel topology, owing to their enormous potential applications as functional materials, such as in microelectronics,¹ luminescent materials,² heterogeneous catalyses,³ gas separation and storage,⁴ nonlinear optics¹c,⁵ and molecular magnetism.⁶ The structural diversity of such solid materials is deeply influenced by many factors, such as pH value, molar ratio of reactants, solvents, temperature, 25 counterions, and the coordination modes of organic ligands or metal ions.¹8 Rational selection of characteristic polycarboxylate ligands is one key factor in the construction of desired CPs. Biphenyltetracarboxylic acid, such as 2,2',3,3'-biphenyltetracarboxylic acid,² 2,2',4,4'-biphenyltetracarboxylic acid,¹0 2,2',5,5'-biphenyltetracarboxylic acid,¹1 2,2',6,6'-biphenyltetracarboxylic acid,¹2 3,3',4,4'-biphenyltetracarboxylic acid¹3 and 3,3',5,5'-biphenyltetracarboxylic acid,¹4 have been proven as good candidates for the syntheses of various CPs, due to their rich coordination modes. To the best of our knowledge, no attention was given to CPs based on the 30 polycarboxylate ligand, 2,3',4,5'-biphenyltetracarboxylic acid, which may be a good candidate for the construction of CPs with new topology and useful property. In view of the above considerations, we chose 2,3',4,5'-biphenyltetracarboxylic acid as a polycarboxylate ligand to generate novel CPs. Herein, we report four new CPs: {[Cu_{2.5}(μ₃-OH¹)(bptc⁴)(4,4'-bpy)(H₂O)₅]·5H₂O}_n(1), {[Cu₂(bptc⁴)(H₂O)₄]·4H₂O)₅]·5H₂O}_n(2), {[Co_{1.5}(Hbptc³)(1,4-bib)_{0.5}(H₂O)₅]·2H₂O}_n(3), and {[Ni₂(bptc⁴)(1,4-bib)_{1.5}(H₂O)₅]·5H₂O}_n(4).

^a Key Laboratory of Aerospace Materials and Performance (Ministry of Education), School of Materials Science and Engineering, Beihang University, No.37, Xueyuan Road, Beijing 100191, China. E-mail: <u>qiaojinzhong@nuc.edu.cn</u>.

^b Department of Chemistry, North University of China, Taiyuan 030051, China. E-mail: Hutuopingsx@126.com.

[†] Electronic Supplementary Information (ESI) available: Additional Figures, excitation spectra, hydrogen bond geometry and X-ray crystallographic data, CCDC 980968, 981706, 981699 and 1018785 for 1-4.



Scheme 1. Coordination Modes of the bptc⁴⁻ and the Hbptc³⁻ in Complexes 1-4

Experimental section

5 The chemicals of 2,3',4,5'-biphenyltetracarboxylic acid, 4,4'-bpy, 1,4-bis(1-imidazolyl)benzene were purchased from Jinan Henghua Sci. & Tec. Co. Ltd and other reagents were commercially available. All chemicals were of analytical grade as obtained and used as received. Elemental analyses for C, H and N were performed on a Vario MACRO cube elemental analyzer. The IR spectra were recorded from KBr pellets in the range from 4000 to 400 cm⁻¹ on a FTIR-8400S spectrometer. Thermal measurements were carried on a ZCT-A thermal analyzer from room temperature to 800 °C with a heating rate of 10 °C/min under nitrogen atmosphere. Powder X-ray diffraction data were collected on a Rigaku D/Max-2500PC diffractometer with Cu Kα radiation (λ=1.5406 Å) over the 2θ range of 5-50° at room temperature. Luminescence spectra for the solid samples were recorded on a EDINBURGH FLSP920 fluorescence spectrophotometer. The variable-temperature magnetic susceptibility measurements were performed on a Quantum Design SQUID MPMS XL-7 instruments in the temperature range of 2-300 K and under the field of 1000 Oe.

15 Syntheses of the complexes

Synthesis of {[Cu_{2.5}(μ₃-OH)(bptc⁴)(4,4'-bpy) (H₂O)]·1.5H₂O}_n (1). A mixture of Cu(NO₃)₂·3H₂O (0.1 mmol, 24.2 mg), H₄bptc (0.05 mmol, 16.5 mg), 4,4'-bpy (0.05 mmol, 7.8 mg), NaOH (0.2 mmol, 8 mg) and H₂O (10 mL) was stirred for 1 h and sealed in a 25 mL Teflon-lined stainless-steel container. The container was heated to 130 °C and held at this temperature for 72 h. It was then cooled to 30 °C at a rate of 5 °C·h⁻¹. Green crystals were collected in 75% yield (based on Cu). Anal. Calc. for 20 C₅₂H₄₀Cu₅N₄O₂₃ (1406.62): C, 44.40; H, 2.87; N, 3.98. Found: C, 42.86; H, 3.21; N, 3.85. IR (cm⁻¹): 3427(s), 1609(vs), 1570(vs), 1539(s), 1413(s), 1375(vs), 1359(vs), 1213(m), 1171(w), 1132(w), 1102(w), 1071(w), 1046(w), 1015(w), 820(m), 796(w), 768(s), 723(m), 704(w), 643(w).

Synthesis of {[Cu₂(bptc⁴)(H₂O)₄]·4H₂O}₁(2). A mixture of Cu(NO₃)₂·3H₂O (0.1 mmol, 24.2 mg), H₄bptc (0.05 mmol, 16.5 mg), NaOH (0.2 mmol, 8 mg) and H₂O (10 mL) was stirred for 1 h and sealed in a 25 mL Teflon-lined stainless-steel container.

25 The container was heated to 130 °C and held at this temperature for 48 h. It was then cooled to 30 °C at a rate of 5 °C·h⁻¹. Blue crystals were collected in 65% yield (based on Cu). Anal. Calc. for C₁₀H₂₂Cu₂O₁₀ (597.43): C, 32.16; H, 3.71. Found: C, 31.32; H, 3.98. IR (cm⁻¹): 3409(vs), 3229(s), 1616(s), 1589(s), 1437(s), 1419(s), 1383(vs), 1288(m), 1269(m), 1118(vw), 1103(w), 771(m), 732(m), 667(m), 487(w)

Synthesis of {[Co_{1.5}(Hbptc³-)(1,4-bib)_{0.5}(H₂O)₅]·2H₂O}_n (3). A mixture of Co(NO₃)₂·6H₂O (0.1 mmol, 29.1 mg), H₄bptc (0.05 30 mmol, 16.5 mg), 1,4-bib (0.05 mmol, 10.5 mg), NaOH (0.1 mmol, 4 mg) and H₂O (10 mL) was stirred for 1 h and sealed in a 25 mL Teflon-lined stainless-steel container. The container was heated to 90 °C and held at this temperature for 48 h. It was then cooled to 30 °C at a rate of 5 °C·h⁻¹. Pink crystals were collected in 58% yield (based on Co). Anal. Calc. for C₄₄H₅₂Co₃N₄O₃₀ (1293.62): C, 40.85; H, 4.05; N, 4.33. Found: C, 40.97; H, 4.10 N, 4.34. IR (cm⁻¹): 3389(vs), 3140(vs), 1700(s), 1611(s), 1524(vs), 1490(s), 1410(vs), 1362(vs), 1307(vs), 1267(s), 1169(m), 1134(m), 1104(m), 1065(s), 963(m), 937(m), 928(m), 914(m), 824(s), 35 763(s), 689(s), 668(s), 656(s), 539(s), 472(s)

Synthesis of $\{[Ni_2(bptc^4-)(1,4-bib)_{1.5}(H_2O)_5]\cdot 5H_2O\}_n$ (4). A mixture of $Ni(NO_3)_2\cdot 6H_2O$ (0.1 mmol, 29.1 mg), H_4bptc (0.05 mmol, 16.5 mg), 1,4-bib (0.05 mmol, 10.5 mg), NaOH (0.2 mmol, 8 mg) and H_2O (10 mL) was stirred for 1 h and sealed in a 25

mL Teflon-lined stainless-steel container. The container was heated to 130 °C and held at this temperature for 72 h. It was then cooled to 30 °C at a rate of 5 °C·h⁻¹. Green crystals were collected in 50% yield (based on Ni). Anal. Calc. for $C_{34}H_{41}N_6Ni_2O_{18}$ (939.11): C, 43.48; H, 4.40; N, 8.95. Found: C, 42.77; H, 4.29; N, 8.83. IR (cm⁻¹): 3348(vs), 1606(s), 1533(vs), 1437(s), 1375(vs), 1310(s), 1267(s), 1133(w), 1110(w), 1068(s), 962(m), 941(m), 838(m), 786(s), 753(s), 712(s), 694(s), 668(s), 653(s), 542(s), 5484(m)

X-ray crystallography

Single-crystal XRD data were collected on a Bruker Apex II CCD diffractometer with graphite-monochromated Cu Kα radiation source (λ= 1.54184 Å) for complex 1 and Mo Kα radiation source (λ= 0.71073 Å) for complexes 2-4 at 293(2) K. Absorption corrections were applied using the multiscan technique. All the structures were solved by direct method of the SHELXS-97 and refined by the 10 full-matrix least-squares techniques using the SHELXL-97. Nonhydrogen atoms were refined with anisotropic temperature parameters. The hydrogen atoms of organic ligands were refined as rigid groups. The approximate positions of the hydrogen atoms for water molecules, obtained from a difference Fourier map, were restrained to ideal configuration of the water molecule and fixed in the final stages of refinements. The detailed crystallographic data and refinement parameters are collected in Table 1. Selected bond lengths and angles for 1-4 are summarized in Table S1(ESI†). Topological analyses for complexes 1, 2 and 4 were performed using the program 15 package TOPOS. 16

Table 1. Crystal data and structure refinements for Compounds 1-4

Compound	1	2	3	4
Empirical formula	C ₅₂ H ₄₀ Cu ₅ N ₄ O ₂₃	C ₁₆ H ₂₂ Cu ₂ O ₁₆	C ₄₄ H ₅₂ Co ₃ N ₄ O ₃₀	C ₃₄ H ₄₁ N ₆ Ni ₂ O ₁₈
Formula weight	1406.62	597.43	1293.62	939.11
Crystal system	triclinic	monoclinic	triclinic	monoclinic
Space group	$P\overline{1}$	$P2_1/c$	$\overline{P1}$	C2/c
a (Å)	10.8509(5)	13.757(3)	7.3730(4)	22.1280(9)
b (Å)	11.1660(7)	20.753(5)	13.0724(7)	14.5817(4)
c (Å)	12.6776(7)	7.8600(19)	13.8570(8)	28.0830(12)
α (°)	107.269(5)	90.00	100.721(5)	90.00
β (°)	95.042(4)	91.660(5)	101.817(5)	116.316(5)
γ (°)	115.812(5)	90.00	98.064(5)	90.00
$V(\mathring{\mathbf{A}}^3)$	1277.63(14)	2243.1(10)	1262.16(12)	8122.3(5)
Z	1	4	1	8
$D_{\rm Calc.}$ (g/cm ³)	1.820	1.754	1.697	1.533
$\mu(\text{mm}^{-1})$	3.110	1.975	1.079	1.010
T(K)	293(2)	293(2)	293(2)	293(2)
θ range (°)	3.774-70.42	1.48-28.67	3.02-25.00	3.10-25.00
Data/Parameters	4775/419	5744/366	4417/435	7169/625
F(000)	703.0	1196.0	661.0	3880.0
$R_{\rm int}$	$R_{\rm int} = 0.0232$	$R_{\rm int}=0.0546$	$R_{\rm int} = 0.0359$	$R_{\rm int}=0.0546$
Final R indices $[I > 2\sigma(I)]$	$R_1 = 0.0416$	$R_1 = 0.0471$	$R_1 = 0.0626$	$R_1 = 0.0533$
	$wR_2 = 0.1127$	$wR_2 = 0.1037$	$wR_2 = 0.1581$	$wR_2 = 0.1278$
R indices (all data)	$R_1 = 0.0527$	$R_1 = 0.0850$	$R_1 = 0.0855$	$R_1 = 0.0836$
	$wR_2 = 0.1219$	$wR_2 = 0.1187$	$wR_2 = 0.1779$	$wR_2 = 0.1495$
Goof	1.054	0.994	1.021	1.042

Results and discussion

Crystal structure of $\{[Cu_{2.5}(\mu_3-OH^-)(bptc^{4-})(4,4'-bpy)(H_2O)]\cdot 1.5H_2O\}_n$ (1).

Single-crystal diffraction analysis reveals that complex 1 crystallizes in triclinic system, P1 space group. The asymmetric unit contains two and a half crystallographically independent Cu(II) ions, one bptc⁴⁻ ligand, one 4,4'-bpy ligand, one coordinated water molecule, one μ_3 -OH⁻ ion, and one and a half lattice water molecules(Fig. 1a). The bpte⁴⁻ is completely deprotonated and shows μ_6 - η_1 : η_2 : η_2 : η_1 coordination mode (model 1 in Scheme 1). The Cu1 ion, which resides on the crystallographic inverse center(site occupancy factor(SOF) = 1/2), is hexa-coordinated by six oxygen atoms: two from two bpte⁴⁻ ligands, two from two coordinated water molecules and two from two μ_3 -OH⁻ anions(Fig. S1, ESI†). The Cu2 ion is penta-coordinated by four oxygen atoms, which are from three bptc⁴⁻ ligands and one μ_3 -OH⁻ anion, and one nitrogen atom from one 4,4'-bpy ligand. The Cu3 ion is located in a distorted tetrahedral environment with τ_4 =0.47,¹⁷ surrounded by three oxygen atoms, which belong to two bptc⁴⁻ ligands and one μ_3 -OH⁻ anion, and one nitrogen atom from one 4,4'-bpy ligand. One Cu1 ion, two Cu2 ions and two Cu3 ions ,which are bridged by two μ_3 -OH⁻ anions, form a {Cu₅O₂} secondary building unit(SBU) (Fig. 1b). The bond lengths of the Cu-O bonds are in the range of 1.935(2) Å ~2.301(3)Å and the Cu-N bond distances are in the range of 1.967(3) Å ~2.031(3) Å. The dihedral angle between the two benzene rings of the bptc⁴⁻ ligand is 46.09°.

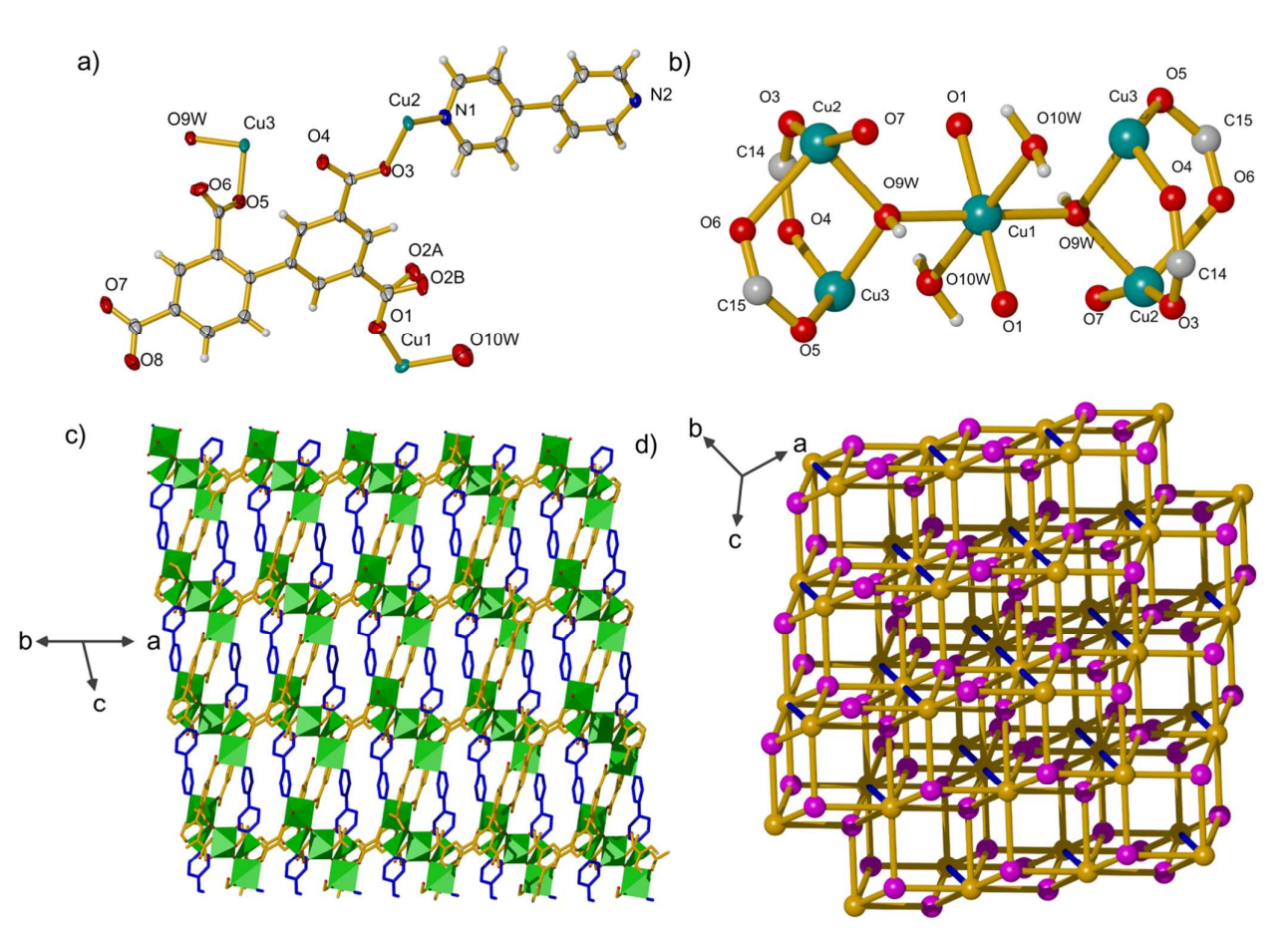


Fig. 1 (a) The asymmetric unit of complex 1 with thermal ellipsoids at 50% probability level. (b) Schematic view of the metal cluster (c) View of the 3D

framework along the [110] direction with hydrogen atoms omitted for clarity (Gold bonds: bptc⁴⁻ ligands; Dark blue bonds: 4,4'-bpy ligands). (d) Schematic view of the 3D network exhibiting a (4,10)-connected deh1 net with the point Schläfli symbol of $\{3\cdot4^5\}_2\{3^4\cdot4^{12}\cdot5^{10}\cdot6^{14}\cdot7^3\cdot8^2\}$ (pink nodes: bptc⁴⁻ ligands; golden nodes: $\{Cu_3O_2\}$ clusters; blue rods: 4,4'-bpy ligands).

Each bptc⁴⁻ ligand connects six Cu(II) ions to form a 3D framework(Fig. 1c), which is stabilized by 4,4'-bpy ligands. There are one-dimensional channels along the [111] direction(Fig. S2, ESI†), in which uncoordinated water molecules reside. With guest water molecules being omitted, the results of PLATON calculations show that the void volume is 11.2 % of the crystal volume (143.2 ų out of the 1277.6 ų unit cell volume). The topological analysis was adopted to simplify the structure. If we view the bptc⁴⁻ ligands as 4-connected nodes, the $\{Cu_5O_2\}$ clusters as 10-connected nodes, and the 4,4'-bpy ligands as μ_2 -linkers respectively, each bptc⁴⁻ ligand is linked with four $\{Cu_5O_2\}$ clusters, and each $\{Cu_5O_2\}$ cluster is connected with eight bptc⁴⁻ ligands and two $\{Cu_5O_2\}$ clusters(Fig. 1d). The overall framework can be defined as a (4,10)-connected deh1 net with the point Schläfli symbol of $\{3\cdot4^5\}_2\{3^4\cdot4^{12}\cdot5^{10}\cdot6^{14}\cdot7^3\cdot8^2\}$.

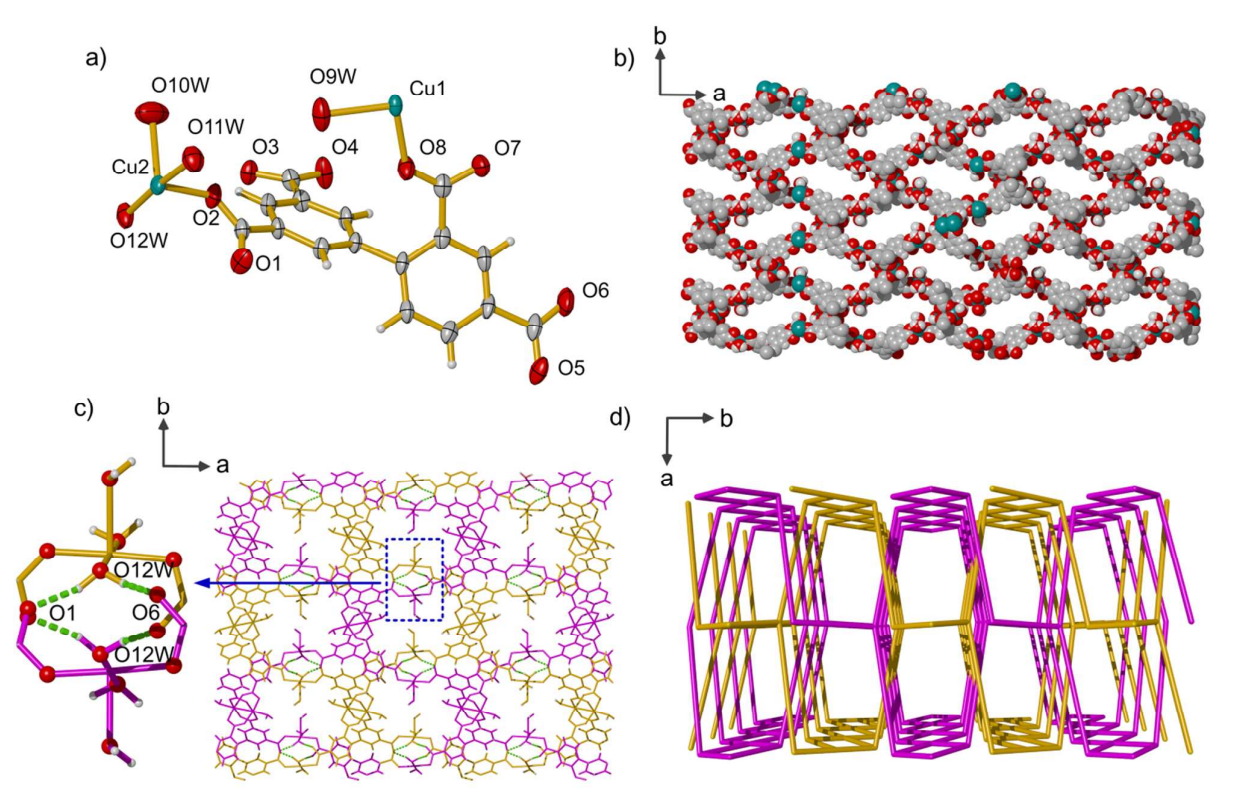


Fig. 2 (a) The asymmetric unit of complex 2 with thermal ellipsoids at 50% probability level. (b) View of the 3D framework with large one-dimensional channels along the [001] direction. (c) Two interpenetrated 3D nets linking with strong hydrogen bonds(green dashed bonds). (d) View of the simplified interpenetrated 3D nets.

Crystal structure of {[Cu₂(bptc⁴⁻)(H₂O)₄]·4H₂O}_n (2)

X-ray crystallographic analysis shows that compound 2 crystallizes in the monoclinic system, $P2_1/c$ space group. The asymmetric unit contains two crystallographically independent Cu(II) ions, one bptc⁴⁻ ligand, four coordinated water molecules and four lattice water molecules(Fig. 2a). The bptc⁴⁻ ligands show the same coordination mode as the ones in complex 1 (model 2

in Scheme 1). The Cu1 ion is hexa-coordinated by another Cu1 ion, five oxygen atoms from four bptc⁴⁻ ligands and one water molecule (Fig. S3, ESI †). The Cu2 ion is penta-coordinated by five oxygen atoms from two bptc⁴⁻ ligands and three water molecules. The bond lengths of the Cu-O bonds are in the range of 1.900(3) Å ~ 2.374(4) Å and the Cu-Cu bond distance is 2.6183(11) Å. The dihedral angle between the benzene rings of the bptc⁴⁻ ligand is 60.176°, which indicates that the bptc⁴⁻ ligand is seriously distorted and unsymmetrical.

Two Cu1 ions bridged by carboxyl oxygen atoms form a binuclear metal cluster, which is connected with four bptc⁴⁻ ligands through μ_4 coordination mode. The Cu2 ion is connected with two bptc⁴⁻ ligands and shows μ_2 mode. A 3D polymeric network is formed by connecting bptc⁴⁻ ligands with Cu2 ions and binuclear Cu1 clusters, containing large one-dimensional channels along the *c* axis (Fig. 2b). The entire structure is composed of two interpenetrated nets, which are linked by strong hydrogen bonds of O12W ··· O1(2.6735 Å) and O12W ··· O6(2.7164 Å)(Fig. 2c and Table S2 for hydrogen bond geometry data, ESI†). Both interpenetrated nets occupy each other's cavities and the rest of cavities are filled in by guest water molecules. Omitting the guest water molecules, the calculations using the software PLATON show that the void volume is 18.4 % of the crystal volume (413.4 ų out of the 2243.1 ų unit cell volume). From the topology view, we can view the Cu2 ions as 2-connected linkers, the bptc⁴⁻ ligands as 4-connected nodes, and the binuclear Cu1 clusters as 4-connected nodes. Fig. 2d shows the simplified interpenetrated 3D nets, and each of them can be viewed as a (4,4)-connected mog Moganite network with the point Schläfli symbol of $\{4.6^4.8\}_2\{4^2.6^2.8^2\}$ (Fig. S4, ESI†).

Crystal structure of $\{[Co_{1.5}(Hbptc^{3-})(1,4-bib)_{0.5}(H_2O)_5]\cdot 2H_2O\}_n$ (3)

There are one and a half crystallographically independent Co(II) cations, one Hbptc³⁻ ligand, a half 1,4-bib ligand, five coordinated water molecules and two lattice water molecules in the asymmetric unit of compound 3(Fig. 3a). The Co1 ion, which is located on the mirror(SOF = 1/2), is hexa-coordinated by four oxygen atoms from four water molecules and two nitrogen atoms from two 1,4-bib ligands. The Co2 ion is also hexa-coordinated by six oxygen atoms, which are from two bptc⁴⁻ anions and three water molecules. The Hbptc³⁻ ligand shows μ_2 - η_0 : η_1 : η_0 : η_1 coordination mode(model 3 in Scheme 1) with three hydrogen deprotonated, and the 1,4-bib ligand takes μ_2 - η_1 : η_1 coordination mode. The dihedral angle between the two benzene rings of the Hbptc³⁻ ligand is 50.102°. Each 1,4-bib ligand links two Co1 cations to form a 1D cationic chain, while each Hbptc³⁻ ligand connects two Co2 cations to generate a 1D anionic chain(Fig. 3b). Interestingly, the 1D anionic chains are assembled through abundant strong hydrogen bonds to generate a 3D supermolecular structure with large one-dimensional channels occupied by the 1D cationic chains along the *c* axis(Fig. 3c, Fig. S5 and Table S3 for hydrogen bond geometry data, ESI†).

Crystal structure of $\{[Ni_2(bptc^{4-})(1,4-bib)_{1.5}(H_2O)_5]\cdot 5H_2O\}_n$ (4)

The asymmetric unit of compound 4 contains two crystallographically independent Ni(II) cations, one bptc⁴⁻ ligand, one and a half 1,4-bib ligands, five coordinated water molecules and five lattice water molecules (Fig. 4a). The Ni1 ion is hexa-coordinated by four oxygen atoms, which are from two bptc⁴⁻ anions and two water molecules, and two nitrogen atoms from two 1,4-bib

ligands(Fig. S6, ESI†). The Ni2 ion is also hexa-coordinated by five oxygen atoms, which are from two bptc⁴⁻ anions and three water molecules, and one nitrogen atom from one 1,4-bib ligand. The bptc⁴⁻ ligand shows μ_4 - η_1 : η_1 : η_1 : η_1 : η_1 : η_1 :oordination mode(model 4 in Scheme 1) with four hydrogen completely deprotonated. The bond lengths of the Ni-O bonds range from 2.019(3) Å to 2.144(3) Å and the Ni-N bond distances are in the range of 2.055(4) Å ~ 2.087(4)Å. The dihedral angle between the benzene rings of the bptc⁴⁻ ligand is 60.176°.

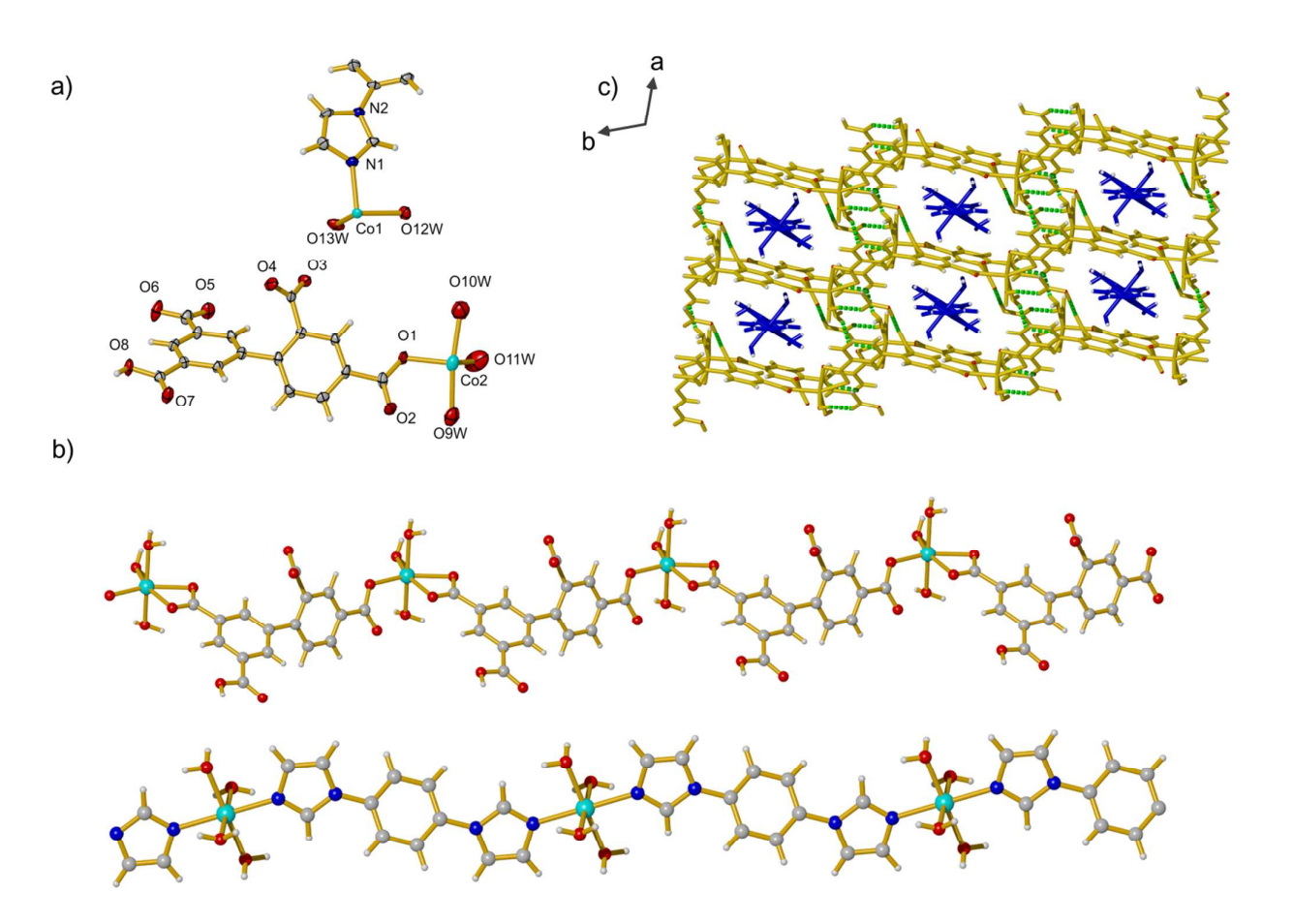


Fig. 3 (a) The asymmetric unit of complex 3 with thermal ellipsoids at 50% probability level. (b) View of the 1D anionic and cationic chains. (c) The 3D supermolecular structure composed of 1D anionic chains with large one-dimensional channels occupied by 1D cationic chains along the *c* axis (green dashed bond: hydrogen bond; blue part: 1D cationic chains).

Each bptc⁴⁻ anion links two Ni1 cations and two Ni2 cations to form a 2D lattice layer(Fig. 4b). The 2D layers are linked by 1,4-bib ligands with μ_2 bridging mode to generate a 3D structure(Fig. 4c). The whole structure contains two interpenetrated networks, which are of the same topological structure (Fig. 4d). From the topology view, each of the interpenetrated networks can be defined as a novel (3,4,4)-connected framework with the point Schläfli symbol {4.6.8} {4.6³.8²} {6⁴.8.10} by denoting the Ni1 cations as 4-connected nodes, the Ni2 cations as 3-connected nodes, the bptc⁴⁻ ligands as 4-connected nodes , and 1,4-bib ligands as 2-connected linkers respectively(Fig. S7, ESI†).

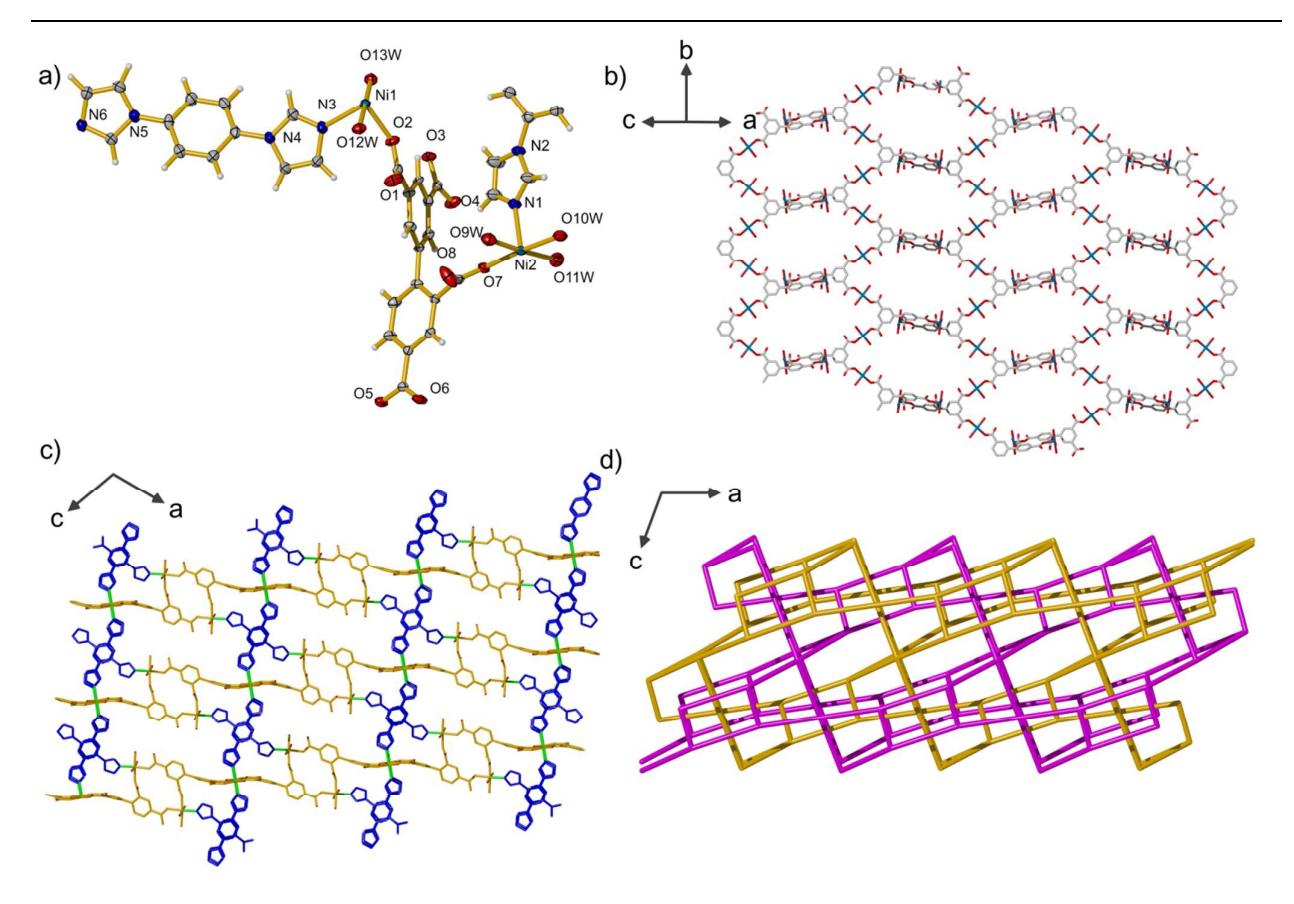


Fig. 4 (a) The asymmetric unit of complex 4 with thermal ellipsoids at 50% probability level. (b) View of the 2D lattice with hydrogen atoms omitted for clarity. (c) The 3D structure with the 1,4-bib ligands bridging 2D lattice and hydrogen atoms omitted for clarity (Gold parts: 2D lattice; Dark blue parts: 1,4-bib ligands; Green bonds: N-Ni bonds). (d) Schematic view of the two interpenetrated nets.

Thermal analyses and PXRD patterns

In order to check the phase purity, the PXRD patterns of complexes 1-4 were checked at room temperature. The peak positions of the simulated and observed PXRD patterns are in agreement with each other, demonstrating the good phase purity of these complexes(Fig. 5).

TG analyses of complexes 1-4 were performed under nitrogen atmosphere with a heating rate of 10 °C min⁻¹(Fig. 6). The TG curve for 1 shows a gradual weight loss below 170 °C, which can be ascribed to the removal of lattice water molecules (observed: 3.95% and calculated: 3.84%). Further, the weight loss observed from 170 °C to 220 °C indicates the removal of coordinated water molecules (observed: 2.54% and calculated: 2.55%). The dramatic weight loss occurs at 280 °C, corresponding to the thermal decomposition of the framework. For compound 2, the weight loss below 120 °C can be attributed to the loss of lattice water molecules (observed: 11.40% and calculated: 12.05%). Further the weight loss observed from 120 °C to 290 °C indicates the removal of coordinated water molecules (observed: 11.10% and calculated: 12.05%). The weight loss, corresponding to thermal decomposition, begins above 290 °C. The initial weight loss of complex 3 is about 18.50% below 240 °C, owing to the loss of water molecules (calculated: 19.48%); The second weight loss is about 4.70% from 240 °C to 330 °C, which can be attributed to the release of one CO molecule (calculated: 4.33%). The framework begins to collapse at 370 °C. For compound 4, the weight loss

below 150 °C can be attributed to the loss of lattice water molecules and coordinated water molecules (observed: 18.60%; calculated: 19.17%). The second weight loss occurs above 370 °C with a result of thermal decomposition.

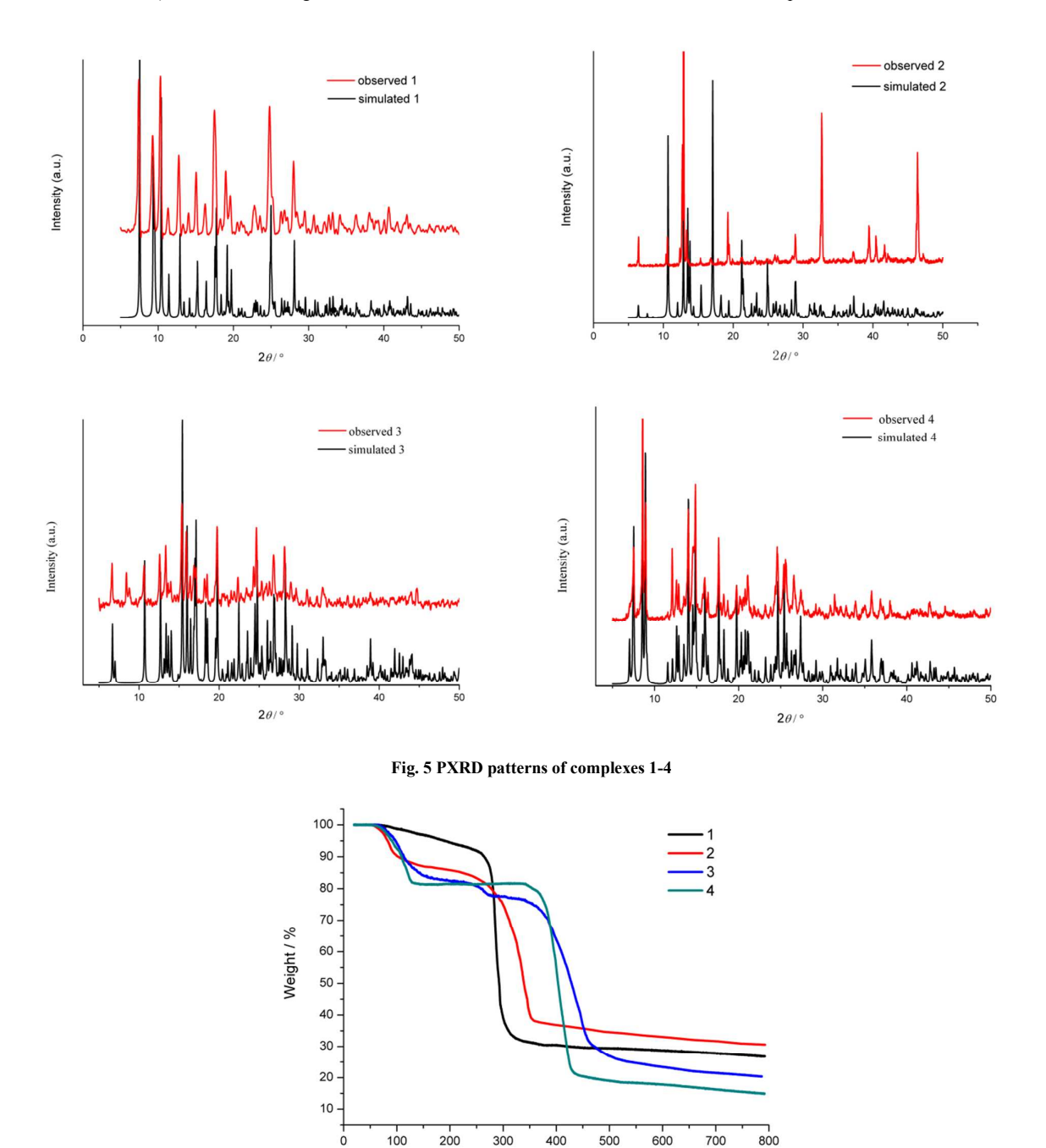


Fig. 6 TG curves of complexes 1-4

Temperature /

 $^{\circ}$ C

Photoluminescent properties

The photoluminescent spectra of complexes 3, 4 and the free H_4 bptc ligand in the solid state at room temperature were investigated(Fig.7 for the emission spectra and Fig. S8 for the excitation spectra, ESI†). The H_4 bptc ligand displays an emission band at 406 nm upon excitation at 341 nm, which may be assigned to the π^* -n or π^* - π transition^{11f}. The complex 3 exhibits two emission bands at 415 and 431(shoulder peak) nm, and the complex 4 shows an emission band at 449 nm upon excitation at λ =350

nm, respectively. Compared with the emission spectrum of H₄bptc, red shifts of 9 nm, 25 nm(shoulder peak) for 3 and 43 nm for 4 were observed, probably due to the metal-to-ligand charge-transfer transition.

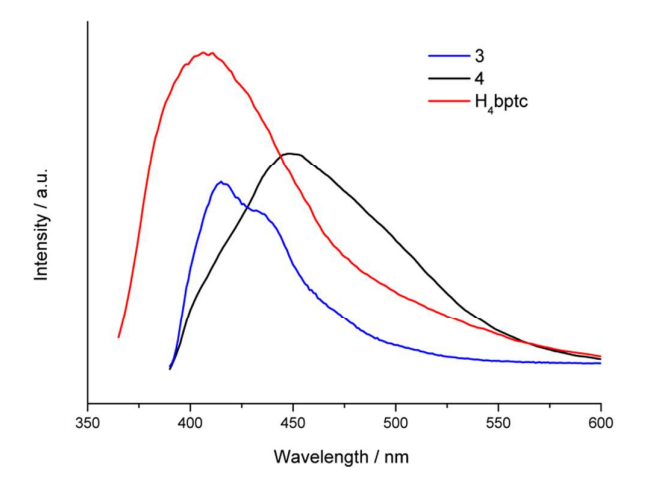


Fig.7 The emission spectra of compound 3, 4 and H4bptc ligand at room temperature.

Magnetic properties

Solid state magnetic susceptibility measurements for 1 and 2 were performed in the range of 2-300 K under a field of 1000 Oe. Plots of $\chi_{\rm M} T$ and $\chi_{\rm M}^{-1} vs T$ for 1 and 2, where $\chi_{\rm M}$ is the molar magnetic susceptibility, are shown in Fig. 8 and Fig. 9.

For 1, at 300 K, the $\chi_M T$ value is 1.829 cm³ K mol⁻¹, which is slightly lower than the calculated value of 1.875 cm³ K mol⁻¹ for five spin-only Cu(II) ions (S=1/2, g=2.0), suggesting the presence of the antiferromagnetic interactions in the 3D net. Upon lowering the temperature, the $\chi_M T$ value gradually decreases from 1.829 cm³ K mol⁻¹ and reaches a minimum value of 1.694 cm³ K mol⁻¹ at 65 K. Then the $\chi_M T$ value increases abruptly to a maximum 2.133 cm³ K mol⁻¹ at ca. 5 K, which probably indicates ferromagnetic interactions between the {Cu₅O₂} clusters. As the temperature is further lowered, the $\chi_M T$ value again decreases to 2.066 cm³ K mol⁻¹ at ca. 2 K. The $\chi_M^{-1} vs T$ curve is well fitted by the Curie-Weiss law above 75 K with the Curie constant of 1.884 cm³ K mol⁻¹ and the Weiss temperature of -7.938 K, respectively. The negative Weiss value is indicative of antiferromagnetic interactions between the neighbouring Cu(II) ions, which is possibly due to the short Cu-Cu distances of 3.134 Å ~3.689 Å. From the Curie constant of 1.884 cm³ K mol⁻¹, it can be concluded that the experimental Lande factor at room temperature corresponds to g=2.005.

For 2, at 300 K, the $\chi_{\rm M}T$ value is 0.523 cm³ K mol⁻¹, which is lower than the calculated value of 0.75 cm³ K mol⁻¹ for two spin-only Cu(II) ions (S=1/2, g=2.0), suggesting the presence of the antiferromagnetic interactions in the 3D net. Upon lowering the temperature, the $\chi_{\rm M}T$ value gradually decreases from 0.523 cm³ K mol⁻¹ and reaches a value of 0.384 cm³ K mol⁻¹ at 70 K. Then the $\chi_{\rm M}T$ value increases very slowly to 0.387 cm³ K mol⁻¹ at ca. 36 K, which probably indicates weak ferromagnetic interactions. As the temperature is further lowered, the $\chi_{\rm M}T$ value again decreases to 0.192 cm³ K mol⁻¹ at ca. 2 K. The $\chi_{\rm M}^{-1}$ vs T curve is well fitted by the Curie-Weiss law above 120 K with the Curie constant of 0.672 cm³ K mol⁻¹ and the Weiss temperature of -83.53 K, respectively. The negative Weiss value is indicative of strong antiferromagnetic interactions between the neighbouring Cu(II) ions, which is possibly due to a Cu/Cu short distance of 2.618 Å. From the Curie constant of 0.672 cm³ K mol⁻¹, it can be concluded that the experimental Lande factor at room

temperature corresponds to g=1.893.

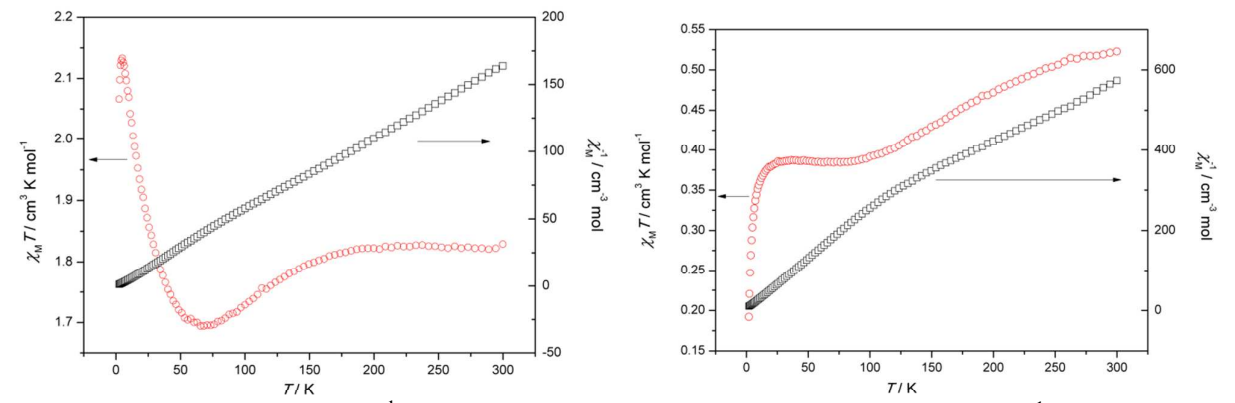


Fig. 8 Temperature dependence of $\chi_{\rm M} T$ and $\chi_{\rm M}^{-1}$ for complex 1.

Fig. 9 Temperature dependence of $\chi_{\rm M}T$ and $\chi_{\rm M}^{-1}$ for complex 2.

Conclusions

In summary, four new CPs, $\{[Cu_3(\mu_3-OH)(bptc^4)(4,4^2-bpy)(H_2O)]\cdot 1.5H_2O\}_n$ (1), $\{[Cu_2(bptc^4)(H_2O)_4]\cdot 4H_2O\}_n$ (2), $\{[Co_{1.5}(Hbptc^3)(1,4-bib)_{0.5}(H_2O)_5]\cdot 2H_2O\}_n$ (3), and $\{[Ni_2(bptc^4)(1,4-bib)_{1.5}(H_2O)_5]\cdot 5H_2O\}_n$ (4), were synthesized and characterized. Complex 1 shows a 3D framework with one-dimensional channels along the [111] direction, while complex 2 consists of two interpenetrated 3D structures. To the best of our knowledge, complex 3 exhibits an interesting 3D supermolecular structure, in which the 1D anionic chains are assembled through hydrogen bonds to form a 3D supermolecular framework with large one-dimensional channels occupied by 1D cationic chains along the *c* axis. Compound 4 contains two interpenetrated nets of a novel (3,4,4)-connected topology, with the point Schläfli symbol of $\{4.6.8\}\{4.6^3.8^2\}\{6^4.8.10\}$. Complexes 1 and 2 exhibit antiferromagnetic behaviour. In addition, the photoluminescent analyses indicate that complexes 3 and 4 are potential luminescent materials.

Author information

Corresponding Author

*E-mail: hutuopingsx@126.com

Acknowledgments

The authors gratefully acknowledge financial support by the International Science & Technology Cooperation Program of China (No. 2011DFA51980), the International Science & Technology Cooperation Program of Shanxi Province (No. 2011DFA51980) and the International Scientific and Technological Cooperation Projects of Shanxi Province (No. 2011081022).

References

- (a)M. Sadakiyo, H. Kasai, K. Kato, M. Takata and M. Yamauchi, J. Am. Chem. Soc., 2014, 136, 1702; (b)M. Yoon, K. Suh, S. Natarajan and K. Kim, Angew. Chem. Int. Ed., 2013, 52, 2688; (c)Z. Yin, Q.-X. Wang and M.-H. Zeng, J. Am. Chem. Soc., 2012, 134, 4857.
- (a) X. J. Zhao, J. H. Yang, Y. Liu, P. F. Gao and Y. F. Li, RSC Adv., 2014, 4, 2573; (b) Q. Tang, S. Liu, Y. Liu, D. He, J. Miao, X. Wang, Y. Ji and Z. Zheng, Inorg. Chem., 2014, 53, 289; (c) Y. Cui, Y. Yue, G. Qian and B. Chen, Chem. Rev., 2012, 112, 1126; (d) Y. Cui, H. Xu, Y. Yue, Z. Guo, J. Yu, Z. Chen, J. Gao, Y. Yang, G. Qian and B. Chen, J. Am. Chem. Soc., 2012, 134, 3979; (e) J. Rocha, L. D. Carlos, F. A. Almeida Paz and D. Ananias, Chem. Soc. Rev., 2011, 40, 926; (f) L.-L. Han, Z.-H. Li, J.-S.

- Chen, X.-P. Wang and D. Sun, *Cryst. Growth Des.*, 2014, **14**, 1221; **(g)**D. Sun, Z.-H. Yan, V. A. Blatov, L. Wang and D.-F. Sun, *Cryst. Growth Des.*, 2013, **13**, 1277; **(h)**L. Zhang, F. Liu, Y. Guo, X. Wang, J. Guo, Y. Wei, Z. Chen and D. Sun, *Cryst. Growth Des.*, 2012, **12**, 6215; **(i)**Z.-J. Lin, L.-W. Han, D.-S. Wu, Y.-B. Huang and R. Cao, *Cryst. Growth Des.*, 2012, **13**, 255.
- 3. (a)J. M. Falkowski, T. Sawano, T. Zhang, G. Tsun, Y. Chen, J. V. Lockard and W. Lin, *J. Am. Chem. Soc.*, 2014, 136, 5213; (b)K. Manna, T. Zhang and W. Lin, *J. Am. Chem. Soc.*, 2014, 136, 6566; (c)H. R. Moon, D.-W. Lim and M. P. Suh, *Chem. Soc. Rev.*, 2013, 42, 1807; (d)Q.-L. Zhu, J. Li and Q. Xu, *J. Am. Chem. Soc.*, 2013, 135, 10210; (e)M. Yoon, R. Srirambalaji and K. Kim, *Chem. Rev.*, 2012, 112, 1196; (f)A. Dhakshinamoorthy and H. Garcia, *Chem. Soc. Rev.*, 2012, 41, 5262; (g)C. Wang, Z. Xie, K. E. deKrafft and W. Lin, *J. Am. Chem. Soc.*, 2011, 133, 13445.
- (a)Z.-J. Lin, Y.-B. Huang, T.-F. Liu, X.-Y. Li and R. Cao, *Inorg. Chem.*, 2013, 52, 3127; (b)H. He, H. Ma, D. Sun, L. Zhang, R. Wang and D. Sun, *Cryst. Growth Des.*, 2013, 13, 3154; (c)R. Wang, Z. Wang, Y. Xu, F. Dai, L. Zhang and D. Sun, *Inorg. Chem.*, 2014, 53, 7086; (d)J. Cui, Y. Li, Z. Guo and H. Zheng, *Chem. Commun.*, 2013, 49, 555; (e)J.-R. Li, J. Sculley and H.-C. Zhou, *Chem. Rev.*, 2012, 112, 869; (f)M. P. Suh, H. J. Park, T. K. Prasad and D.-W. Lim, *Chem. Rev.*, 2012, 112, 782; (g)T. A. Makal, J.-R. Li, W. Lu and H.-C. Zhou, *Chem. Soc. Rev.*, 2012, 41, 7761; (h)Z. R. Herm, J. A. Swisher, B. Smit, R. Krishna and J. R. Long, *J. Am. Chem. Soc.*, 2011, 133, 5664; (i)X. Gu, Z.-H. Lu, H.-L. Jiang, T. Akita and Q. Xu, *J. Am. Chem. Soc.*, 2011, 133, 11822.
- 5. (a)C. Wang, T. Zhang and W. Lin, *Chem. Rev.*, 2012, **112**, 1084; (b)C. Wang, J.-L. Wang and W. Lin, *J. Am. Chem. Soc.*, 2012, **134**, 19895.
- (a)S. Biswas, H. S. Jena, A. Adhikary and S. Konar, *Inorg. Chem.*, 2014, 53, 3926; (b)Z. Xu, W. Meng, H. Li, H. Hou and Y. Fan, *Inorg. Chem.*, 2014, 53, 3260; (c)M. Wriedt, A. A. Yakovenko, G. J. Haider, A. V. Prosvirin, K. R. Dunbar and H.-C. Zhou, *J. Am. Chem. Soc.*, 2013, 135, 4040; (d)D.-S. Li, J. Zhao, Y.-P. Wu, B. Liu, L. Bai, K. Zou and M. Du, *Inorg. Chem.*, 2013, 52, 8091; (e)D.-F. Weng, Z.-M. Wang and S. Gao, *Chem. Soc. Rev.*, 2011, 40, 3157.
- (a)B. Chen, N. W. Ockwig, F. R. Fronczek, D. S. Contreras and O. M. Yaghi, *Inorg. Chem.*, 2004, 44, 181; (b)X. Bao, P.-H. Guo, W. Liu, J. Tucek, W.-X. Zhang, J.-D. Leng, X.-M. Chen, I. y. Gural'skiy, L. Salmon, A. Bousseksou and M.-L. Tong, *Chem. Sci.*, 2012, 3, 1629; (c)S. Wang, Y. Peng, X. Wei, Q. Zhang, D. Wang, J. Dou, D. Li and J. Bai, *Crystengcomm*, 2011, 13, 5313; (d)Z. Lin and M.-L. Tong, *Coord. Chem. Rev.*, 2011, 255, 421; (e)H.-S. Choi and M. P. Suh, *Angew. Chem. Int. Ed.*, 2009, 48, 6865; (f)S. Yang, X. Lin, A. J. Blake, K. M. Thomas, P. Hubberstey, N. R. Champness and M. Schroeder, *Chem. Commun.*, 2008, 6108.
- 8. (a)J.-L. Liu, W.-Q. Lin, Y.-C. Chen, J.-D. Leng, F.-S. Guo and M.-L. Tong, *Inorg. Chem.*, 2013, 52, 457; (b)L. Fan, X. Zhang, D. Li, D. Sun, W. Zhang and J. Dou, *Crystengcomm*, 2013, 15, 349; (c)P.-H. Guo, J.-L. Liu, Z.-M. Zhang, L. Ungur, L. F. Chibotaru, J.-D. Leng, F.-S. Guo and M.-L. Tong, *Inorg. Chem.*, 2012, 51, 1233; (d)C.-X. Chen, Q.-K. Liu, J.-P. Ma and Y.-B. Dong, *J. Mater. Chem.*, 2012, 22, 9027; (e)X. Zhao, D. Sun, S. Yuan, S. Feng, R. Cao, D. Yuan, S. Wang, J. Dou and D. Sun, *Inorg. Chem.*, 2012, 51, 10350; (f)A. H. Shelton, I. V. Sazanovich, J. A. Weinstein and M. D. Ward, *Chem. Commun.*, 2012, 48, 2749.
- (a)H.-H. Li, N. Ma and K.-H. Li, J Inorg Organomet P, 2012, 22, 1320; (b)C.-Z. Mei, W.-W. Shan and B.-T. Liu, Chinese J. Struct. Chem., 2011, 30, 1173; (c)C.-Z. Mei, J.-X. Wang and W.-W. Shan, Chinese J. Struct. Chem., 2011, 30, 1194; (d)S. Zang, Y. Su, Y.-Z. Li, J. Lin, X. Duan, Q. Meng and S. Gao, Crystengcomm, 2009, 11, 122.
- (a) Y.-H. Su, F. Luo, H. Li, Y.-X. Che and J.-M. Zheng, *Crystengcomm*, 2011, 13, 44; (b) Z.-R. Pan, J. Xu, X.-Q. Yao, Y.-Z. Li, Z.-J. Guo and H.-G. Zheng, *Crystengcomm*, 2011, 13, 1617; (c) H. Tian, K. Wang, Q.-X. Jia, Q. Sun, Y. Ma and E.-Q. Gao, *Cryst. Growth Des.*, 2011, 11, 5167; (d) J. Jia, M. Shao, T. Jia, S. Zhu, Y. Zhao, F. Xing and M. Li, *Crystengcomm*, 2010, 12, 1548; (e) T. Jia, S. Zhu, M. Shao, Y. Zhao and M. Li, *Inorg. Chem. Commun.*, 2008, 11, 1221.
- (a) S.-Q. Guo, D. Tian, Y.-H. Luo, X. Chen and H. Zhang, J. Solid State Chem., 2013, 205, 110; (b) S. Guo, D. Tian, Y. Luo and H. Zhang, J. Coord. Chem., 2012, 65, 308; (c) D. Tian, Y. Pang, S. Guo, X. Zhu and H. Zhang, J. Coord. Chem., 2011, 64, 1006; (d) S.-Q. Guo, D. Tian, X. Zheng and H. Zhang, Inorg. Chem. Commun., 2011, 14, 1876; (e) D. Tian, Y.-H. Zhou, L. Guan, X.-F. Zhu, Y. Pang and H. Zhang, Chinese J. Struct. Chem., 2011, 30, 120; (f) D. Tian, Y. Pang, Y.-H. Zhou, L. Guan and H. Zhang, Crystengcomm, 2011, 13, 957.
- 12. (a) C.-Z. Mei, G.-R. Yang and K.-H. Li, *Chinese J. Struct. Chem.*, 2013, 32, 225; (b) B. Li, S.-Q. Zang, C. Ji, H.-W. Hou and T. C. W. Mak, *Cryst. Growth Des.*, 2012, 12, 1443; (c) Z. Yang, J. Liu, X.-Q. Liang, Y. Jiang, T. Zhang, B. Han, F.-X. Sun and L.

- Liu, *Inorg. Chem. Commun.*, 2012, **16**, 92; (d)C.-Z. Mei, W.-W. Shan and B.-T. Liu, *Z Naturforsch B*, 2011, **66**, 654; (e)C.-Z. Mei, W.-W. Shan and B.-T. Liu, *Spectrochim. Acta, Part A*, 2011, **81**, 764.
- (a)G.-H. Pan, S.-H. Xu, W.-J. Xu, P. Liang, W.-M. Tian and Z.-J. Huang, J. Chem. Crystallogr., 2014, 44, 312; (b)G.-D. Feng, L. Jiang, Q. Chen, D.-S. Yang, M.-J. Wang, Z.-X. Li and X.-L. Luo, Chinese J. Struct. Chem., 2013, 32, 45; (c)W. Wei, S. Chen, Q. Wei, G. Xie, Q. Yang and S. Gao, Microporous Mesoporous Mater., 2012, 156, 202; (d)S. Zhang, G. Xie, Y. Zou, S. Chen and S. Gao, J. Coord. Chem., 2012, 65, 1062; (e)P.-k. Chen, Y. Qi, Y.-x. Che and J.-m. Zheng, Crystengcomm, 2010, 12, 720; (f)L.-X. Sun, Y. Qi, Y.-M. Wang, Y.-X. Che and J.-M. Zheng, Crystengcomm, 2010, 12, 1540; (g)S. Deng, N. Zhang, W. Xiao and C. Chen, Inorg. Chem. Commun., 2009, 12, 157; (h)S. Zhu, H. Zhang, M. Shao, Y. Zhao and M. Li, Transition Met. Chem., 2008, 33, 669; (i)G.-P. Yang, Y.-Y. Wang, H. Wang, C.-J. Wang, G.-L. Wen, Q.-Z. Shi and S.-M. Peng, J. Mol. Struct., 2008, 888, 366; (j)D. Weng, X. Zheng, L. Li, W. Yang and L. Jin, Dalton Trans., 2007, 4822; (k)G.-P. Yang, Y.-Y. Wang, L.-F. Ma, J.-Q. Liu, Y.-P. Wu, W.-P. Wu and Q.-Z. Shi, Eur. J. Inorg. Chem., 2007, 3892.
- (a)Q. Zhang and J. n. M. Shreeve, *Angew. Chem. Int. Ed.*, 2014, 53, 2540; (b)L. Zhu, J. Gao and Z. An, *J. Mol. Struct.*, 2014, 1067, 239; (c)M. L. Foo, S. Horike, J. Duan, W. Chen and S. Kitagawa, *Cryst. Growth Des.*, 2013, 13, 2965; (d)J. Qian, F. Jiang, D. Yuan, X. Li, L. Zhang, K. Su and M. Hong, *J. Mater. Chem. A.*, 2013, 1, 9075; (e)F. Yang, Q. Zheng, Z. Chen, Y. Ling, X. Liu, L. Weng and Y. Zhou, *Crystengcomm*, 2013, 15, 7031; (f)B. L. Chen, N. W. Ockwig, F. R. Fronczek, D. S. Contreras and O. M. Yaghi, *Inorg. Chem.*, 2005, 44, 181; (g)D. Sun, L.-L. Han, S. Yuan, Y.-K. Deng, M.-Z. Xu and D.-F. Sun, *Cryst. Growth Des.*, 2013, 13, 377.
- M. B. Bushuev, B. A. Selivanov, N. V. Pervukhina, D. Y. Naumov, L. A. Sheludyakova, M. I. Rakhmanova, A. Y. Tikhonov and S. V. Larionov, J. Coord. Chem., 2014, 67, 611.
- 16. L. Sarkisov, R. L. Martin, M. Haranczyk and B. Smit, J. Am. Chem. Soc., 2014, 136, 2228.
- 17. L. Yang, D. R. Powell and R. P. Houser, *Dalton Trans.*, 2007, 955.
- 18. (a) A. L. Spek, J. Appl. Crystallogr., 2003, 36, 7; (b) A. L. Spek, Utrecht University, Utrecht, The Netherlands, 2001, 20.
- 19. (a) V. Blatov, *J. Appl. Crystallogr*, 2000, **33**, 1193; (b) Z.-Y. Li, Y. Zhang, C.-W. Zhang, L.-J. Chen, C. Wang, H. Tan, Y. Yu, X. Lo and H.-B. Yang, *J. Am. Chem. Soc.*, 2014, **136**, 8577; (c) V. Blatov, M. O'keeffe and D. Proserpio, *CrystEngComm*, 2010, **12**, 44.